#### **Research Article**

Benjaporn Noppradit, Setsiri Chaiyosburana, Nutthaphol Khupsathianwong, Weena Aemaeg Tapachai, Yupa Wattanakanjana, and Apichat Phengdaam\*

# Green synthesis of silver nanoparticles using Saccharum officinarum leaf extract for antiviral paint

https://doi.org/10.1515/gps-2023-0172 received September 06, 2023; accepted November 15, 2023

Abstract: In this study, silver nanoparticles (AgNPs) were synthesized via an eco-friendly approach using an extract from sugarcane leaves (Saccharum officinarum). The optimal synthesis conditions were determined to be a pH of 10, yielding AgNPs with an average size of 11.7 ± 2.8 nm. This was substantiated by UV-vis spectral analysis, transmission electron microscopy, and field emission transmission electron microscope coupling with selected area electron diffraction. The synthesized AgNPs exhibited notable antibacterial efficacy against two prominent pathogens, namely Staphylococcus aureus and Escherichia coli, with minimum inhibitory concentration values of 20 and 2.5 ppm, respectively. Further extending the applications of AgNPs, they were successfully integrated into architectural paints at varying concentrations to create antiviral coatings. The addition of AgNPs influenced several properties of the paints, including viscosity, hiding power, and color characteristics. Notably, our findings revealed that the antiviral paint containing 80 ppm of AgNPs effectively hindered virus propagation, exhibiting a remarkable reduction of over 90% when compared to the control, measured by 50% tissue culture infectious dose.

\* Corresponding author: Apichat Phengdaam, Division of Physical Science, Faculty of Science, Prince of Songkla University, Hat Yai, Songkhla 90110, Thailand, e-mail: apichat.p@psu.ac.th

**Benjaporn Noppradit:** Department of Pharmacognosy and Pharmaceutical Botany, Faculty of Pharmaceutical Sciences, Prince of Songkla University, Hat Yai, Songkhla 90110, Thailand

**Setsiri Chaiyosburana:** NIST International School, 36 Sukhumvit Soi 15, Klongtoey-nua, Wattana, Bangkok 10110, Thailand

**Nutthaphol Khupsathianwong:** Technopreneurship and Innovation Management Program, Graduate School, Chulalongkorn University, Bangkok 10330, Thailand

**Weena Aemaeg Tapachai, Yupa Wattanakanjana:** Division of Physical Science, Faculty of Science, Prince of Songkla University, Hat Yai, Songkhla 90110, Thailand

**Keywords:** AgNPs, *Saccharum officinarum*, MIC, architectural paints, TCID50

#### 1 Introduction

The current COVID-19 pandemic has been a global wake-up call in ways never before imagined. People have now changed how they live and incorporate hygienic practices into their daily lives to avoid catching the virus [1,2]. Regularly washing our hands, wearing masks, and avoiding crowds do not provide sufficient protection. Because the coronavirus (SARS-CoV-2) can remain viable on surfaces for several hours to days, the chance of infection increases after touching those surfaces [3]. Although viruses are relatively easy to destroy using simple cleansers, such as sanitizer or detergent, it is difficult to sanitize surfaces continuously, and they are usually quickly contaminated again. Thus, many people want to use antimicrobial paint on many surfaces for safety and to create hygiene zones while navigating this pandemic [4].

The paint is mostly desired for use in high-cleanliness areas, including healthcare, hospitality, office, and educational environments, but it can also be used in residential environments. Due to high demand, several paint manufacturers have tried to develop effective antiviral formulas. Antiviral paint serves as an intelligent delivery mechanism aimed at mitigating the potential hazards associated with contact of contaminated high-touch surfaces [5–7]. Generally, the paint contains a readily available metal that has been used since ancient times to reduce harmful germs, such as copper. Silver has been known to have effective bactericidal properties for centuries and was widely used to reduce infections in burns, open wounds, and chronic ulcers [8,9].

At present, nanotechnology is associated with various medical and hygiene applications [10]. Silver nanoparticles (AgNPs), with their potential as antibiotic alternatives, can interact with and permeate bacterial cell membranes. The escalating bacterial resistance to antibiotics, largely attributed to their overuse or misuse, signals a concerning era for commonly employed antibiotics [11]. AgNPs have recently become a topic of interest because of their biological properties, including their antifungal, antiviral, anti-inflammatory, antiangiogenetic, and antiplatelet activity [12]. Moreover, AgNPs have various potential applications in non-medical areas, such as food, cosmetics, electronics, engineering, and pharmacology [13–17]. The increasingly high-paced research has yielded improved properties based on specific characteristics, such as size, distribution, and morphology [18].

Conventional AgNP syntheses are relatively expensive and environmentally unfriendly. Because some of the chemicals used for nanoparticle synthesis and stabilization are toxic, the synthesis by-products are not eco-friendly. Thus, the increasing demand for ecologically benign methods of synthesizing nanoparticles or green chemical processes has sparked a growing interest in utilizing biological materials for green synthesis and environmentally friendly technologies [19–27]. This aligns with the objectives of the United Nations Sustainable Development Goals, which aim to mitigate climate change through the zero-waste utilization of agricultural by-products [28].

One of the most popular plants used to synthesize AgNPs is sugarcane (Saccharum officinarum) [16]. In particular, sugarcane leaves are available for the synthesis procedure throughout the year. To use more industrial waste, the sugarcane bagasse has also been used [17]. An extract from fresh sugarcane leaves provides a simple, cost-effective, eco-friendly, stable, and efficient route for synthesizing AgNPs [16,29]. Furthermore, the AgNPs from this green synthesis procedure using fresh sugarcane leaves showed effective antibacterial and antifungal activity against multiple drug-resistant hospital isolates [16]. In another report, the AgNPs were prepared using a Soxhlet extract of the sugarcane bagasse as a reducing and capping agent. In addition, good antimicrobial activity was observed when these AgNPs were used against Gram-negative and Gram-positive bacteria [29]. This new green synthesis method supports the valuable utilization of biomass for the synthesis of metal nanoparticles.

To leverage waste material for value creation, sugarcane leaves represent a promising option for the green synthesis of AgNPs. This choice is substantiated by the eco-friendly and substantial post-harvest waste generated, which contributes significantly to the production of PM 2.5 through combustion processes [30]. This approach not only addresses air pollution concerns in agricultural contexts but also offers environmentally friendly means of utilizing green AgNPs to mitigate the risk of infection transmission

among people. Although the green-synthesized AgNPs exhibited strong antibacterial activity, another desirable property of AgNPs is antiviral activity. Numerous objects incorporating silver in daily life have been found to provide antiviral activity [31,32]. However, a few studies have focused on the viral inhibitory effect of surface-coating AgNPs in paints. Therefore, our research goal was to develop green AgNPs synthesized using sugarcane leaves combined with paint products to control viruses. This research yields a smart delivery system to reduce the risk of exposure to contaminated high-touch surfaces.

#### 2 Materials and methods

#### 2.1 Chemicals and materials

Silver nitrate (AgNO<sub>3</sub>) and sodium hydroxide (NaOH) were purchased from Merck. The glassware was soaked in 0.5 M HNO<sub>3</sub> before it was cleaned with detergent and rinsed with deionized (DI) water. All chemicals were of analytical grade and were used as received. DI water was used as a solvent throughout this study.

#### 2.2 Sugarcane leaf extraction

Fresh sugarcane leaves (*Saccharum officinarum*) were harvested from local farms in Kanchanaburi Province, Thailand, during November and December. These freshly harvested leaves were then subjected to a 1-week drying process under direct sunlight. The leaves were cut into short strips and rinsed with DI water three times to remove impurities. A 500 g portion of sugarcane leaf was prepared by placing the cut leaves within a semi-permeable cloth bag and submerging it in 22 L of hot DI water. The reaction was conducted at 80°C for 2 h with continuous stirring. The brown solution was then cooled to room temperature and filtered using Whatman No. 1 filter paper.

#### 2.3 Synthesis of AqNPs

Silver ions (500 ppm) from  $AgNO_3$  were prepared in DI water.  $AgNO_3$  was completely dissolved and mixed with the sugarcane leaf extract in a 1:1 ratio. Next, 1 M NaOH was added to adjust the pH of the solution to 6, 8, 10, and 12; the reaction was conducted at room temperature with

10 min of constant stirring. During the reaction, the brown sugarcane leaf extract solution changed to a clear brownishyellow color. AgNPs reached a final concentration of 250 ppm, and the solution was used as the stock solution for subsequent procedures.

# 2.4 Characterization of AqNPs

AgNPs were analyzed using UV-vis spectrophotometry in the wavelength range of 300-700 nm (Genesys 30 UV-Vis Spectrophotometer; Thermo Scientific). Furthermore, the dimensions, morphology, and characteristic crystalline structure of the resulting AgNPs were assessed using transmission electron microscopy (JEM-2100 TEM; JEOL) and field emission transmission electron microscope (Talos F200i FE-TEM; Thermo Fisher Scientific) coupling with selected area electron diffraction (SAED) detector. To obtain molecular bonding information, attenuated total reflection-Fourier transform infrared (ATR-FTIR) spectra of the AgNPs were collected with a diamond probe from 500 to 4,000 cm<sup>-1</sup> (Nicolet iS5 FT-IR Spectrometer; Thermo Scientific).

# 2.5 Antibacterial properties of AqNPs

The antibacterial properties of AgNPs were evaluated using the minimum inhibitory concentration (MIC) protocol provided by the Department of Microbiology, Chulalongkorn University, Thailand. AgNP concentrations (0-40 ppm) were tested against Staphylococcus aureus (S. aureus) and Escherichia coli (E. coli) in Luria-Bertani (LB) broth. A UV-Vis spectrophotometer was used to measure growth inhibition via optical density at 600 nm. The negative and positive controls used AgNP-free and AgNP-containing LB broth, respectively.

#### 2.6 Blending AgNPs in paint

AgNPs at a concentration of 250 ppm were incorporated into 3,000 mL of architectural paint through agitation with 4-blade mixing impellers at 500-800 rpm for 10 min (LaboratoryKreis-Basket-Mill®, Wilhelm Niemann). The AgNP concentrations in the paint, ranging from 60 to 120 ppm, were manipulated by adjusting the volume of the initial AgNP stock solution before mixing. Subsequently, viscometers (CAP 2000 viscometer; BYK and Digital Krebs viscometer (480); Sheen)

and a spectrophotometer (Color i7 spectrophotometer; X-Rite) were employed to assess the viscosity and color characteristics of the resulting antiviral paint.

# 2.7 Antiviral activity of AgNP-containing paint

The antiviral assessment of AgNPs included 50% tissue culture infectious dose (TCID50) provided by Virology Research Services, UK. Specimens were positioned on disks, and a virus solution containing 2 × 10<sup>6</sup> IU·mL<sup>-1</sup> of human coronavirus NL63 was applied with Rhesus Monkey Kidney Epithelial (LLC-MK2) cells serving as the host. Then, the disks were covered by the film. The virus was added to the control as a baseline. After incubation, the film was removed, and the samples were washed to recover the virus. The TCID50 determined the recovered infectious virus quantity.

#### 3 Results and discussion

# 3.1 Effect of pH on AgNP morphology

In agreement with previous investigations, pH is key to the optimal green synthesis of AgNPs. This influence extends beyond the reliance of the reduction potential solely upon the abundance of reducing functional groups inherent in natural sources [33]. The concentrations of the acidic or basic environment impact the initiation of nucleation events needed for the synthesis of AgNPs. This, in turn, increases or decreases the population of AgNPs [34]. Consequently, to exploit this behavior, the pH was changed to 6, 8, 10, and 12 during the incorporation of the sugarcane leaf extract, giving it the capacity to act as a reducing agent. At pH 12, a notable quantity of gray particulates precipitated during the AgNP synthesis, likely due to the elevated ionic strength from the alkaline environment. This subsequently reduced the stability of the system, resulting in a simultaneous coalescence of AgNPs [35]. After this preparatory phase, an in-depth exploration was undertaken using the UV-Vis spectra of colloidal AgNPs (Figure 1).

The absorption behavior of AgNPs surpassed that exhibited by either the AgNO<sub>3</sub> precursor or the sugarcane leaf that acted as the reducing agent. The UV-Vis spectra acquired from the green synthesis at various pH values revealed distinct attributes indicative of AgNPs, marked by a maximal

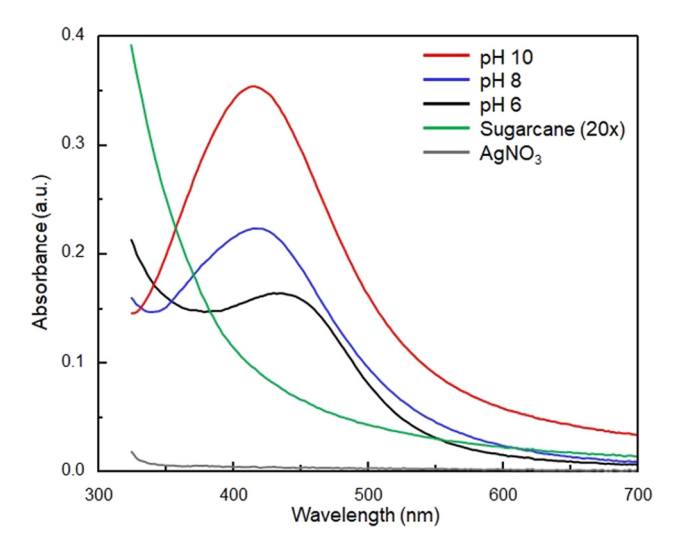


**Figure 1:** UV-Vis spectra of AgNPs via green synthesis at pH 6, 8, and 10 compared with  $AgNO_3$  and sugarcane leaf at  $20 \times$  dilution.

absorption peak within the spectral range of 400–450 nm. The discernible yellow hue of the resulting solution, coupled with a single absorption band within the visible region, corroborates the occurrence of localized surface plasmon resonance (LSPR) characteristics of spherical AgNPs, while the absorption intensity directly shows the population density of AgNPs [36]. Furthermore, notable, blue-shifted spectra were observed, specifically in the context of increasing the pH from 6 to 8 to 10, each yielding maximum absorption peaks

at 430, 420, and 410 nm, respectively. To further investigate this phenomenon, the morphology of AgNPs synthesized at various pH values was studied using TEM (Figure 2).

The TEM analysis revealed the formation of AgNPs during the green synthesis, which was distinct from the sugarcane leaf extract (Figure 2a). Furthermore, a reduction in the average particle size with increasing pH was observed, measuring  $18.2 \pm 5.4$  (Figure 2b),  $13.8 \pm 3.8$  (Figure 2c), and  $11.7 \pm 2.8$  nm (Figure 2d). These results agree with the trend in particle dimensions determined from the LSPR characteristics in the preceding section (Figure 1). These distinctive optical phenomena show that the particle dimensions of AgNPs are influenced by changing the pH of the sugarcane leaf extract, ultimately leading to a reduction in the particle size [37].

To conduct a comprehensive investigation, AgNPs synthesized through the green synthesis process at pH 10 was deliberately chosen. This analysis was carried out employing FE-TEM (Figure 3a). At higher magnification, the atomic structure exhibited characteristics consistent with closely packed arrangements, revealing a *d*-spacing of 0.235 Å. This observation conclusively establishes that the crystal plane (111) corresponds to a face-centered cubic crystal structure of silver [38]. Furthermore, the SAED pattern demonstrates the presence of multiple crystal planes, including (111), (200), (220), (311), and (222) (Figure 3b). These crystal planes were ascertained by comparison with XRD and SAED patterns reported in previous studies of AgNP

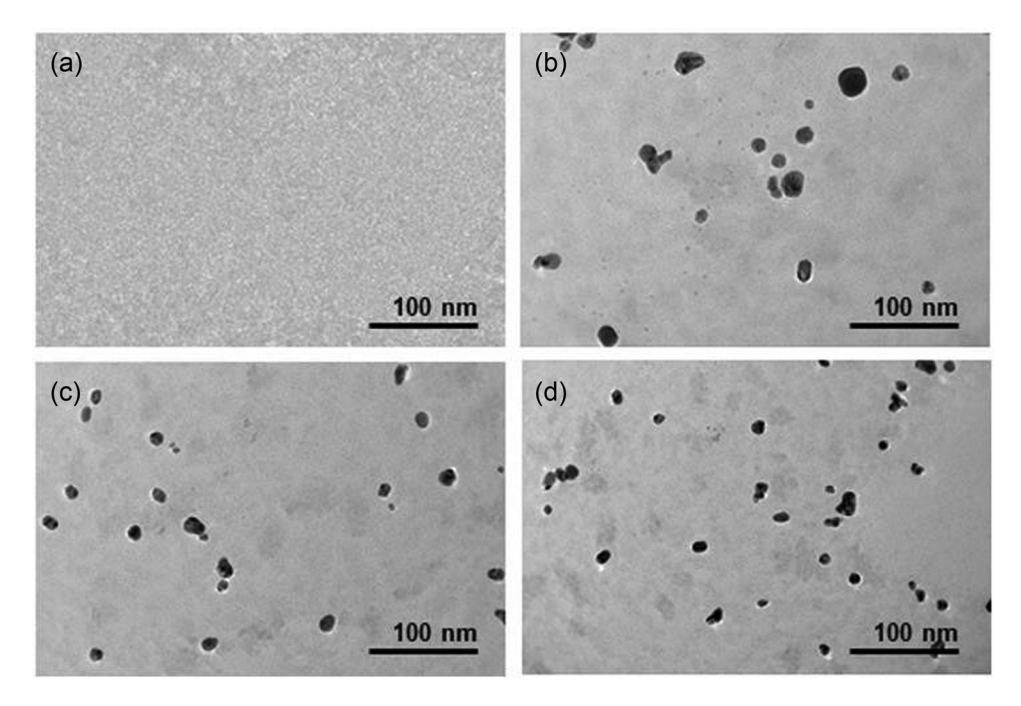


Figure 2: TEM images of (a) the sugarcane leaf extract and AgNPs via green synthesis at pH (b) 6, (c) 8, and (d) 10.

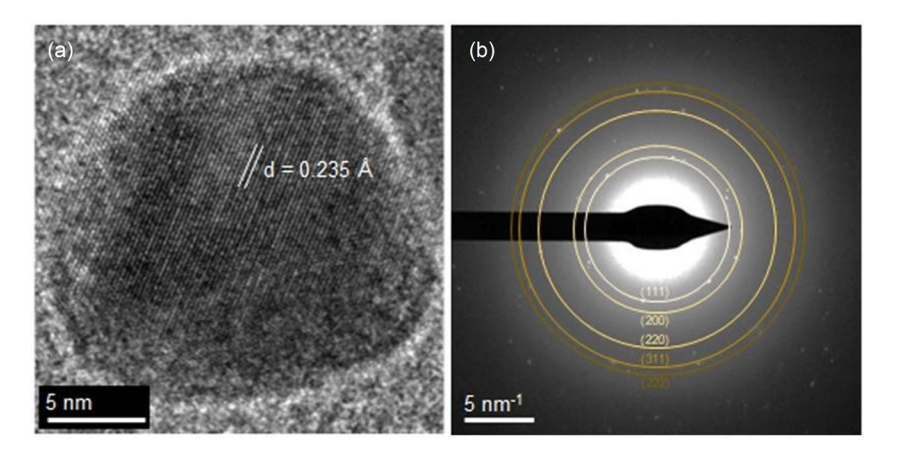


Figure 3: FE-TEM images illustrating (a) AgNPs synthesized via a green synthesis process at pH 10, accompanied by (b) the corresponding SAED pattern.

synthesis [39]. Therefore, the collective evidence derived from spectroscopic, morphological, and crystallographic analyses serves to affirm that the green synthesis process employed herein is indeed capable of yielding AgNPs.

It is generally acknowledged that the growth kinetics of metal nanoparticles are regulated by the reducing power, which is contingent upon the concentration of the reducing agent [40]. Within the environment of sugarcane leaves, the heightened reduction potential inherent in the -NH, -OH, and phenolic groups makes them effective reducing agents, particularly under alkaline conditions [41,42]. Therefore, increasing the alkaline conditions should promote the reduction potential of the sugarcane leaf extract. To better understand this system, the green-synthesized AgNPs at pH 10 were analyzed using ATR-FTIR spectroscopy (Figure S1 and Table S1). This analysis showed a pronounced transmission peak at 941 cm<sup>-1</sup>, assigned to amine and hydroxyl groups, which can act as relatively mild reducing agents [43]. Furthermore, the distinctive functional group of -COO was observed at 1,510 cm<sup>-1</sup>. Numerous studies have shown that carboxylic derivatives can stabilize AgNPs [44,45]. Thus, the sugarcane leaf extract has a dual role as a reducing agent and stabilizer. Subsequently, the AgNPs in this study were synthesized using the sugarcane leaf extract at pH 10, a choice informed by observing the smallest particle size and the highest population density in the ensuing investigations (Figures 1 and 2).

### 3.2 Antibacterial properties of AgNPs

Generally, metal nanomaterials physically interact with prokaryotic cells, disrupting cellular functions, destabilizing the phospholipid bilayer of cells, and inducing cell lysis. They can also bind to cytosolic proteins like DNA, leading to cell death, and generate reactive oxygen species by elevating oxidative stress and cell instability [46,47]. As previously documented, green AgNPs have exhibited notably potent antibacterial properties [48-51]. To preliminarily assess their potential antiviral efficacy, the antibacterial effectiveness of the synthesized AgNPs was evaluated against S. aureus and E. coli in the LB broth. The MIC test was employed as the defining criterion, indicating the lowest concentration of an antimicrobial agent that effectively suppresses visible microbial growth following an incubation period [52]. The MIC tests of AgNPs against the specified bacterial strains (Figure 4) revealed distinct concentrations corresponding to MIC values of 20 ppm for S. aureus and 2.5 ppm for E. coli (Tables S2 and S3). Additionally, MIC values reported in this research emphasize the effectiveness of AgNPs, approximately 10 nm in size, synthesized using both green and conventional methods that involve aggressive chemicals. These nanoparticles exhibited similar efficiency in inhibiting the growth of both S. aureus and E. coli [53]. As previously reported, SARS-CoV-2 has exhibited less susceptibility to AgNPs than E. coli, and S. aureus outside the host environment, as evidenced by comparative assessments of their survival at analogous AgNP concentration levels [53-55]. Therefore, this observation underscores the potential of green AgNPs as a basis for developing antiviral coatings with promising efficacy.

#### 3.3 Properties of paint blended with AqNPs

To synergistically integrate the antiviral attributes of AgNPs within architectural coatings, the physical and optical characteristics of the resultant paints were investigated thoroughly, including parameters such as viscosity, hiding

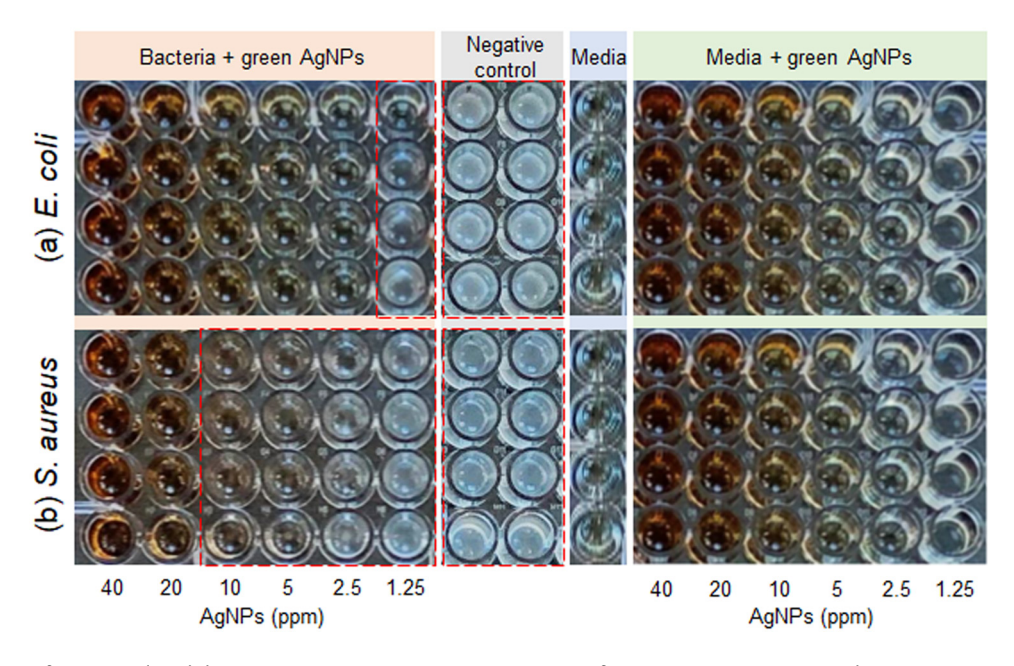


Figure 4: MIC tests for (a) E. coli and (b) S. aureus at AgNP concentrations ranging from 1.25 to 40 ppm over 24 h.

power, and tonal characteristics, with reference to an unmodified control paint sample. The viscosities of the control paint and the 60, 80, 100, and 120 ppm AgNP-incorporated formulations were determined with Krebs and cone-plate viscometers (Figure 5). Due to the inherent thixotropic characteristics of the paint, this viscosity assessment examined the variation in viscosity under shear stress, along with a comprehensive analysis of the distribution of shear rates. This multifaceted viscosity evaluation is particularly relevant to practical applications within painting techniques [56].

This analysis indicates a substantial reduction in viscosity. The linear reduction is correlated with increasing AgNP concentration. The colloidal AgNPs were seamlessly incorporated into the architectural coatings; that is, AgNPs were directly integrated into water-based paints. However, the paint base was diluted by adding colloidal AgNPs suspended in water, which served as the solvent. Adhering to established guidelines for architectural coatings, the viscosity of paints must be within 70–80 KU or 75–100 cP to function correctly in conventional paint application methodologies involving rollers [57]. Additionally, decreasing the paint base concentration impacts coverage efficacy and opacity, aspects that were rigorously assessed [58].

To investigate the impact of dilution on AgNP-infused paint, the hiding power was evaluated utilizing a checker-board-patterned black and white wallpaper (Figure 6). The efficacy of surface coverage decreased when the AgNP

concentrations were 100 and 120 ppm. The diminished concealment capacity observed at elevated AgNP concentration coincides with the lower viscosity values measured previously. Consequently, the effect of dilution is crucial to both the viscosity and hiding power of AgNP-loaded paint formulations.

The effects of adding AgNPs extended beyond surface attributes and included changes in the appearance with varied concentrations of AgNPs. Color changes resulting

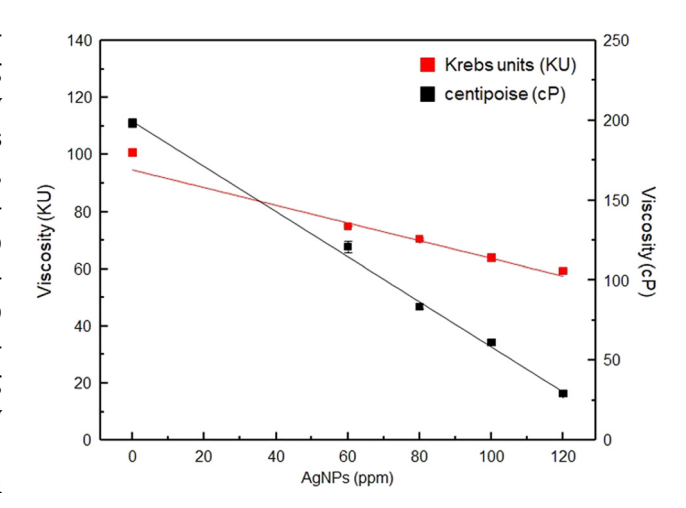


**Figure 5:** The viscosity of architectural paints with varying AgNP concentrations ranging between 0 and 120 ppm, measured by Krebs and cone–plate viscometers.

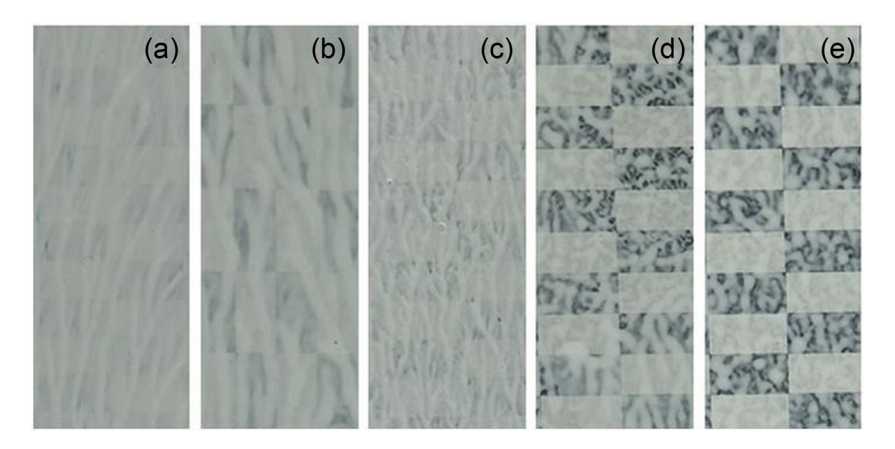


Figure 6: The hiding power of architectural paints with AgNP concentrations of (a) 0, (b) 60, (c) 80, (d) 100, and (e) 120 ppm.

from different AgNP paint concentrations were systematically quantified using the CIE color scale (Table S4). The CIE color scale measurements were subsequently translated into RGB values (Figure 7). Notably, the most elevated RGB values were measured in the control, which contained no AgNPs. When AgNPs were added, the influence of different concentrations on the coloration of the paint was clear, especially when compared to the control conditions. This contrast was particularly discernible in the Hex color variations observed for AgNP concentrations of 100 and 120 ppm.

With increasing AgNP concentration, the RGB values decreased, most likely due to the dilution of the paint. Concomitantly, a positive correlation was observed between the ratio of the red component (R) to the overall RGB value and the increasing AgNP concentration. This phenomenon is

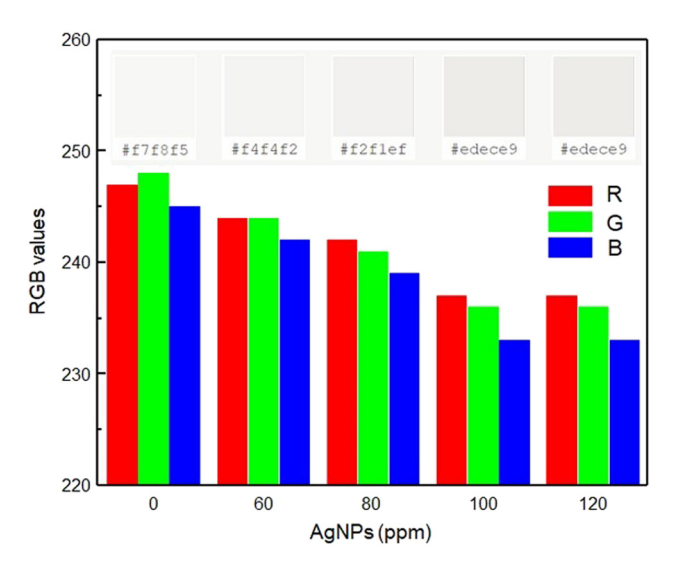


Figure 7: RBG values with inset images of Hex color codes of architectural paints with AgNP concentrations ranging between 0 and 120 ppm.

explained by the vibrant color attributed to the LSPR of AgNPs, particularly the yellow color, which corresponded to an increased R to RGB ratio [59].

Despite the chromatic alterations from the LSPR of AgNPs, the fundamental composition and morphology of AgNPs remained unchanged within the paint. Paints containing increased concentrations of AgNPs should increase efficacy in suppressing a wide spectrum of bacterial agents [60]. Within the paints containing AgNPs, careful selection of AgNP concentration is necessary to attain enhanced antiviral effects. However, AgNP-bearing paints must have physical and optical properties close to those of the control paint. Considering these criteria, an AgNP concentration of 80 ppm was chosen for subsequent antiviral assessments.

# 3.4 Antiviral efficacy of paint containing **AqNPs**

AgNPs exhibit antiviral potential by interacting with viral envelope/surface proteins, blocking viral entry into cells, and disrupting cellular pathways of infection. They can also interact with viral genetic material, target viral replication processes, and interfere with cellular components essential for viral replication [61]. Therefore, AgNPs have a high potential to be included in consuming health care for antiviral properties. In this work, the treated substrate with AgNP paint showed measurable virucidal propensity against human coronavirus NL63, with a contact duration of 24 h. The dilution at which 50% of cells were infected or eradicated (TCID50) was determined using the Reed and Muench method [62]. The quantification of the antiviral activity (R) is given by the following equation:

$$R = Ut - At \tag{1}$$

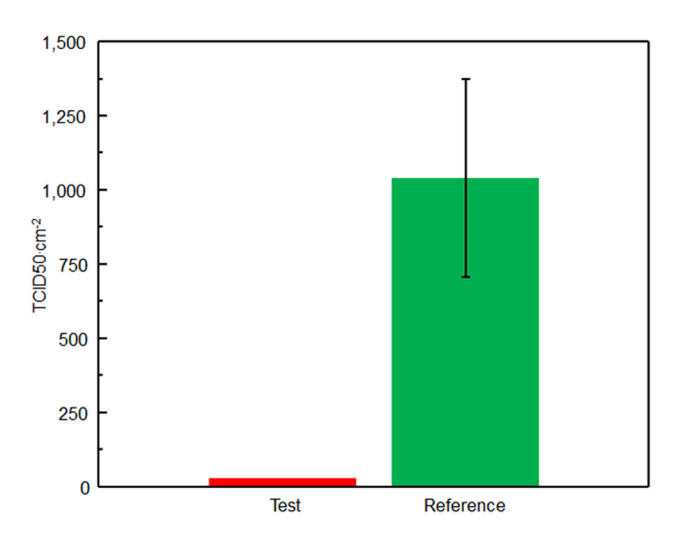


**Figure 8:** The mean TDIC50·cm<sup>-2</sup> values for human coronavirus NL63 following a contact time of 24 h for test and reference control materials.

where Ut represents the average of the logarithm of the number of infectious units recovered from the untreated test specimens after the incubation period, while At represents the average of the logarithm of the number of infectious units recovered from the treated test specimens at the termination of the incubation period [63]. The results of this antiviral test for the AgNP-bearing paint are summarized in Table S5. An R-value greater than or equal to 1 indicates the presence of antiviral activity. In summary, the average recovered titer for the treated material was 2.96 × 10 TDIC50·cm<sup>-2</sup> compared to an average recovered titer of 1.04 × 10<sup>3</sup> TDIC50·cm<sup>-2</sup> for the untreated reference control (see Figure 8). In this study, the antiviral activity is assessed by the R-value. For these data, the calculated Rvalue of 1.55 surpasses the threshold of 1, substantiating the presence of antiviral activity. This observation signifies a reduction of virus propagation exceeding 90% compared to the reference control. This suggests their promising role in antiviral applications and our result validates the robust antiviral efficacy of AgNPs contained within the paint.

#### 4 Conclusions

This study presents an environmentally friendly approach to synthesizing AgNPs using the sugarcane (*Saccharum officinarum*) leaf extract. Optimal synthesis conditions were determined under alkaline pH and enhancing reducing potential. UV-vis spectroscopy, TEM, FE-TEM coupling with SAED, and Fourier transform infrared spectroscopy were used to measure optical, morphological, crystallographic, and molecular properties influenced by pH. AgNPs exhibited

notable antibacterial activity against *S. aureus* and *E. coli*, confirmed by the MIC. The integration of AgNPs into architectural paints for antiviral coatings was explored while adhering to architectural paint standards. Significantly, the formulation containing 80 ppm AgNPs showcased remarkable antiviral potential, achieving over 90% reduction in virus propagation compared to the reference control, as determined by the TCID50. This discovery shows that sugarcane leaf extract-derived AgNPs are potent antibacterial agents and essential components for advanced antiviral architectural paints. The research contributes to advancing nanomaterial synthesis and holds promising implications for prospective applications.

**Acknowledgement:** The authors would like to thank B.N. Brothers Company Limited, Thailand, for materials, instruments, and kind advice.

**Funding information**: This work (Number 364005) was financially supported by the Faculty of Science, Prince of Songkla University, Thailand.

**Author contributions**: Benjaporn Noppradit: conceptualization, methodology, validation, formal analysis, and writing – original draft. Setsiri Chaiyosburana: methodology, validation, and investigation. Nutthaphol Khupsathianwong: methodology, validation, and investigation. Weena Aemaeg Tapachai: resources and methodology. Yupa Wattanakanjana: resources and methodology. Apichat Phengdaam: resources, methodology, validation, investigation, writing – review & editing, supervision, and funding acquisition.

**Conflict of interest**: The authors state no conflict of interest.

**Data availability statement**: All data generated or analyzed during this study are included in this published article and its supplementary information file.

#### References

- Sarmiento PJD. Changing landscapes of death and burial practices: public health response in time of COVID-19 pandemic. J Public Health. 2020;43(2):e267–8.
- [2] Tabari P, Amini M, Moghadami M, Moosavi M. International public health responses to COVID-19 outbreak: A rapid review. Iran J Med Sci. 2020;45(3):157–69.
- 3] Otter J, Donskey C, Yezli S, Douthwaite S, Goldenberg S, Weber D. Transmission of SARS and MERS coronaviruses and influenza virus in healthcare settings: the possible role of dry surface contamination. J Hosp Infect. 2016;92(3):235–50.

- [4] Nguyen THT, Le HT, Le XTT, Do TTT, Ngo TV, Phan HT, et al. Interdisciplinary assessment of hygiene practices in multiple locations: Implications for COVID-19 pandemic preparedness in Vietnam. Front Public Health. 2021;8:589183.
- Grover N, Douaisi MP, Borkar IV, Lee L, Dinu CZ, Kane RS, et al. Perhydrolase-nanotube paint composites with sporicidal and antiviral activity. Appl Microbiol Biotechnol. 2013;97(19):8813-21.
- Haldar I. Weight AK, Klibanov AM, Preparation, application and testing of permanent antibacterial and antiviral coatings. Nat Protoc. 2007;2(10):2412-7.
- Rakowska PD, Tiddia M, Faruqui N, Bankier C, Pei Y, Pollard AJ, et al. Antiviral surfaces and coatings and their mechanisms of action. Commun Mater. 2021;2(1):53.
- Parikh DV, Fink T, Rajasekharan K, Sachinvala ND, Sawhney APS, Calamari TA, et al. Antimicrobial silver/sodium carboxymethyl cotton dressings for burn wounds. Text Res J. 2016;75(2):134-8.
- Shankar SS, Rai A, Ahmad A, Sastry M. Controlling the optical properties of lemongrass extract synthesized gold nanotriangles and potential application in infrared-absorbing optical coatings. Chem Mater. 2005;17(3):566-72.
- [10] Dos Santos CA, Seckler MM, Ingle AP, Gupta I, Galdiero S, Galdiero M, et al. Silver nanoparticles: therapeutical uses, toxicity, and safety issues. J Pharm Sci. 2014;103(7):1931-44.
- Baran MF, Keskin C, Baran A, Hatipoğlu A, Yildiztekin M, Küçükaydin S, et al. Green synthesis of silver nanoparticles from Allium cepa L. Peel extract, their antioxidant, antipathogenic, and anticholinesterase activity. Molecules. 2023;28(5):2310.
- Wiley BJ, Im SH, Li Z-Y, McLellan J, Siekkinen A, Xia Y. Maneuvering [12] the surface plasmon resonance of silver nanostructures through shape-controlled synthesis. J Phys Chem B. 2006;110(32):15666-75.
- [13] Li W-R, Xie X-B, Shi Q-S, Zeng H-Y, Ou-Yang Y-S, Chen Y-B. Antibacterial activity and mechanism of silver nanoparticles on Escherichia coli. Appl Microbiol Biotechnol. 2009;85(4):1115-22.
- [14] Kaur H, Bhatnagar A, Tripathi SK. Size tunable green synthesis of silver nanoparticles using Trachyspermum Ammi (Ajwain) and their effect on a B cell line. J Nanoeng Nanomanuf. 2013;3(2):154-61.
- [15] Zhang X-F, Liu Z-G, Shen W, Gurunathan S. Silver nanoparticles: synthesis, characterization, properties, applications, and therapeutic approaches. Int | Mol Sci. 2016;17(9):1534.
- [16] Chaudhari PR, Masurkar SA, Shidore VB, Kamble SP. Biosynthesis of silver nanoparticles using Saccharum officinarum and its antimicrobial activity. Micro Nano Lett. 2012;7(7):646-50.
- [17] Mishra A, Sardar M. Rapid biosynthesis of silver nanoparticles using sugarcane bagasse—an industrial waste. J Nanoeng Nanomanuf. 2013;3(3):217-9.
- [18] Singh A, Jain D, Upadhyay MK, Khandelwal N, Verma HN. Green synthesis of silver nanoparticles using Argemone Mexicana leaf extract and evaluation of their antimicrobial activities. Dig J Nanomater Biostruct. 2010;5(2):483-9.
- [19] Raveendran P, Fu J, Wallen SL. Completely "Green" synthesis and stabilization of metal nanoparticles. J Am Chem Soc. 2003;125(46):13940-1.
- [20] Mittal AK, Chisti Y, Banerjee UC. Synthesis of metallic nanoparticles using plant extracts. Biotechnol Adv. 2013;31(2):346-56.
- [21] Yildirim A, Baran MF, Acay H. Kinetic and isotherm investigation into the removal of heavy metals using a fungal-extract-based bionanosorbent. Environ Technol Innov. 2020;20:101076.
- [22] Baran MF, Duz MZ. Removal of cadmium(II) in the aqueous solutions by biosorption of Bacillus licheniformis isolated from soil in

- the area of Tigris River. Int J Environ Anal Chem. 2021;101(4):533-48.
- [23] Keskin C, Baran A, Baran MF, Hatipoğlu A, Adican MT, Atalar MN, et al. Green synthesis, characterization of gold nanomaterials using Gundelia tournefortii leaf extract, and determination of their nanomedicinal (antibacterial, antifungal, and cytotoxic) potential. J Nanomater. 2022;2022:7211066.
- [24] Baran M, Duz M, Uzan S, Dolak İ, Celik K, Kılınç E. Removal of Hq(II) from aqueous solution by Bacillus subtilis ATCC 6051 (B1). I Bioprocess Biotech. 2018;8(4):1-7.
- [25] Hatipoğlu A, Baran A, Keskin C, Baran MF, Eftekhari A, Omarova S, et al. Green synthesis of silver nanoparticles based on the Raphanus sativus leaf aqueous extract and their toxicological/ microbiological activities. Environ Sci Pollut Res. 2023:30:1-13.
- [26] Moradi F, Sedaghat S, Moradi O, Arab Salmanabadi S. Review on green nanobiosynthesis of silver nanoparticles and their biological activities: With an emphasis on medicinal plants. Inorg Nano-Metal Chem. 2021;51(1):133-42.
- Sheikh-Mohseni MH, Sedaghat S, Derakhshi P, Safekordi A. Green biosynthesis of Ni/montmorillonite nanocomposite using extract of Allium jesdianum as the nano-catalyst for electrocatalytic oxidation of methanol. Chin J Chem Eng. 2020;28(10):2555-65.
- Axon S, James D. The UN sustainable development goals: How can **[281** sustainable chemistry contribute? A view from the chemical industry. Curr Opin Green Sustain Chem. 2018;13:140-5.
- [29] Aguilar NM, Arteaga-Cardona F, Estévez JO, Silva-González NR, BenítezSerrano JC, Salazar-Kuri U. Controlled biosynthesis of silver nanoparticles using sugar industry waste, and its antimicrobial activity. J Environ Chem Eng. 2018;6(5):6275-81.
- Silva FS, Cristale J, André PA, Saldiva PH, Marchi MR. PM2. 5 and [30] PM10: The influence of sugarcane burning on potential cancer risk. Atmos Environ. 2010;44(39):5133-8.
- [31] Davies RL, Etris SF. The development and functions of silver in water purification and disease control. Catal Today. 1997;36(1):107-14.
- [32] Silvestry-Rodriguez N, Bright KR, Slack DC, Uhlmann DR, Gerba CP. Silver as a residual disinfectant to prevent biofilm formation in water distribution systems. Appl Environ Microbiol. 2008;74(5):1639-41.
- [33] Tongsakul D, Wongravee K, Thammacharoen C, Ekgasit S. Enhancement of the reduction efficiency of soluble starch for platinum nanoparticles synthesis. Carbohydr Res. 2012;357:90-7.
- [34] Ahmad N, Sharma S. Green synthesis of silver nanoparticles using extracts of Ananas comosus. Green Sustain Chem. 2012;2:141-7.
- [35] Xia Y, Xiong Y, Lim B, Skrabalak SE. Shape-controlled synthesis of metal nanocrystals: simple chemistry meets complex physics? Angew Chem Int Ed. 2009;48(1):60-103.
- [36] Parnklang T, Lertvachirapaiboon C, Pienpinijtham P, Wongravee K, Thammacharoen C, Ekgasit S. H2O2-triggered shape transformation of silver nanospheres to nanoprisms with controllable longitudinal LSPR wavelengths. RSC Adv. 2013;3(31):12886-94.
- [37] Phengdaam A, Nootchanat S, Ishikawa R, Lertvachirapaiboon C, Shinbo K, Kato K, et al. Improvement of organic solar cell performance by multiple plasmonic excitations using mixed-silver nanoprisms. J Sci: Adv Mater Dev. 2021;6(2):264-70.
- [38] Rani P, Kumar V, Singh PP, Matharu AS, Zhang W, Kim K-H, et al. Highly stable AgNPs prepared via a novel green approach for catalytic and photocatalytic removal of biological and non-biological pollutants. Environ Int. 2020;143:105924.

- [39] Cai Y, Piao X, Gao W, Zhang Z, Nie E, Sun Z. Large-scale and facile synthesis of silver nanoparticles via a microwave method for a conductive pen. RSC Adv. 2017;7(54):34041–8.
- [40] Yoo S, Nam DH, Singh TI, Leem G, Lee S. Effect of reducing agents on the synthesis of anisotropic gold nanoparticles. Nano Convergence. 2022;9(1):5.
- [41] Velu M, Lee J-H, Chang W-S, Lovanh N, Park Y-J, Jayanthi P, et al. Fabrication, optimization, and characterization of noble silver nanoparticles from sugarcane leaf (Saccharum officinarum) extract for antifungal application. 3 Biotech. 2017;7:1–9.
- [42] Srikhao N, Kasemsiri P, Lorwanishpaisarn N, Okhawilai M. Green synthesis of silver nanoparticles using sugarcane leaves extract for colorimetric detection of ammonia and hydrogen peroxide. Res Chem Intermed. 2021;47:1269–83.
- [43] Xiong Y, Washio I, Chen J, Cai H, Li Z-Y, Xia Y. Poly (vinyl pyrrolidone): a dual functional reductant and stabilizer for the facile synthesis of noble metal nanoplates in aqueous solutions. Langmuir. 2006;22(20):8563–70.
- [44] Titkov AI, Logutenko OA, Gerasimov EY, Shundrina IK, Karpova EV, Lyakhov NZ. Synthesis of silver nanoparticles stabilized by carboxylated methoxypolyethylene glycols: the role of carboxyl terminal groups in the particle size and morphology. J Incl Phenom Macrocycl Chem. 2019;94(3):287–95.
- [45] Irfan MI, Amjad F, Abbas A, Rehman MFu, Kanwal F, Saeed M, et al. Novel carboxylic acid-capped silver nanoparticles as antimicrobial and colorimetric sensing agents. Molecules. 2022;27(11):3363.
- [46] Gold K, Slay B, Knackstedt M, Gaharwar AK. Antimicrobial activity of metal and metal-oxide based nanoparticles. Adv Ther. 2018;1(3):1700033.
- [47] Hoseini-Alfatemi SM, Karimi A, Armin S, Fakharzadeh S, Fallah F, Kalanaky S. Antibacterial and antibiofilm activity of nanochelating based silver nanoparticles against several nosocomial pathogens. Appl Organomet Chem. 2018;32(5):e4327.
- [48] Acay H, Baran M. Biosynthesis and characterization of silver nanoparticles using king oyster (Pleurotus eryngii) extract: Effect on some microorganisms. Appl Ecol Environ Res. 2019;17(4):9205–14.
- [49] Baran MF. Synthesis and antimicrobial applications of silver nanoparticles from artemisia absinthium plant. Biol Chem Res. 2019;6:96–103.
- [50] Acay H, Baran MF. Investigating antimi crobial activity of silver nanoparticles produc ed through green syn thesis using leaf

- extract of common grape (Vitis Vinifera). Appl Ecol Environ Res. 2019:17(2):4539–46.
- [51] Baran M, Koç A, Uzan S. Synthesis, characterization and antimicrobial applications of silver nanoparticles (AgNPs) with kenger (Gundelia tournefortii) leaf. EJONS. Int J Math Eng Nat Sci. 2018;5:44–52.
- [52] Andrews JM. Determination of minimum inhibitory concentrations. J Antimicrob Chemother. 2001;48(suppl\_1):5–16.
- [53] Agnihotri S, Mukherji S, Mukherji S. Size-controlled silver nanoparticles synthesized over the range 5–100 nm using the same protocol and their antibacterial efficacy. RSC Adv. 2014;4(8):3974–83.
- [54] Tremiliosi GC, Simoes LGP, Minozzi DT, Santos RI, Vilela DCB, Durigon EL, et al. Ag nanoparticles-based antimicrobial polycotton fabrics to prevent the transmission and spread of SARS-CoV-2. bioRxiv. 2020 Jun;2020:152520.
- [55] Jeremiah SS, Miyakawa K, Morita T, Yamaoka Y, Ryo A. Potent antiviral effect of silver nanoparticles on SARS-CoV-2. Biochem Biophys Res Commun. 2020;533(1):195–200.
- [56] Lapasin R, Pricl S, Lapasin R, Pricl S. Rheometry. Rheology of Industrial Polysaccharides: Theory and Applications. NY: Springer; 1995. p. 495–578.
- [57] Committee. Test Method for Consistency of Paints Measuring Krebs Unit (KU) Viscosity Using a Stormer-Type Viscometer. West Conshohocken, PA: ASTM International; 2018.
- [58] Committee. Test method for relative hiding power of paints by the visual evaluation of brushouts. West Conshohocken, PA: ASTM International; 1997.
- [59] Lobregas MOS, Bantang JPO, Camacho DH. Carrageenan-stabilized silver nanoparticle gel probe kit for colorimetric sensing of mercury (II) using digital image analysis. Sens Bio-Sens Res. 2019;26:100303.
- [60] Ciriminna R, Albo Y, Pagliaro M. New antivirals and antibacterials based on silver nanoparticles. ChemMedChem. 2020;15(17):1619–23.
- [61] Rai M, Deshmukh SD, Ingle AP, Gupta IR, Galdiero M, Galdiero S. Metal nanoparticles: The protective nanoshield against virus infection. Crit Rev Microbiol. 2016;42(1):46–56.
- [62] Reed LJ, Muench H. A simple method of estimating fifty per cent endpoints12. Am J Epidemiol. 1938;27(3):493–7.
- [63] Committee, Measurement of antiviral activity on plastics and other non-porous surfaces, in Plastics in general. Vol. ISO 21702. Geneva: International Organization for Standardization; 2019. p. 2019.